Adsorption (2008) 14: 447–455
DOI 10.1007/s10450-008-9117-x

Water vapour adsorption and contrast-modified SAXS in microporous polymer-based carbons of different surface chemistry

Krisztina László · Cyrille Rochas · Erik Geissler

Received: 1 May 2007 / Revised: 5 November 2007 / Accepted: 20 March 2008 / Published online: 8 April 2008

Abstract The adsorption of water vapour on highly microporous activated carbons with different surface chemistry is investigated by small angle X-ray scattering (SAXS) as well as by adsorption isotherms. The water changes the intensity of the SAXS in a way that depends on how the pores are filled. With wetting liquids such as hexane, a pseudo binary model can be assumed in which pore-filling in reciprocal space q is described by a density function $p(q)$. For water, clusters develop, even in the most oxidized carbon, creating a fully ternary system. In the Porod scattering region, however, the final slope is insensitive to the liquid-vapour interfaces. In this region, for the less oxidized samples, $p(q)$ shows reasonable agreement with the adsorption isotherms. At low relative pressure P/P_0, however, the SAXS results indicate a small degree of filling (about 10%) that is not reflected in the isotherms. The highly oxidized sample attains a degree of filling of about 70% that, unlike the corresponding isotherm, is constant for $P/P_0 > 0$. These differences may be due to kinetic effects and/or ageing, involving either redistribution of the water molecules or modifications of the surface groups.

Keywords Activated carbon · Surface treatment · Small angle X-ray scattering · Interfacial properties

K. László (✉)
Department of Physical Chemistry, Budapest University of Technology and Economics, 1521 Budapest, Hungary
e-mail: klaszlo@mail.bme.hu

C. Rochas · E. Geissler
Laboratoire de Spectrométrie Physique CNRS UMR 5588, Université J. Fourier de Grenoble, BP 87, 38402 St. Martin d'Hères Cedex, France

1 Introduction

Since ancient times the high affinity of carbon for a wide diversity of chemical species has established it as a multipurpose adsorbent. Nowadays carbon adsorbents with tailor-made surface area and pore hierarchy have become commercially available (Lozano-Castelló et al. 2001a; Lillo-Ródenas et al. 2001; Dash et al. 2005). In addition to these geometrical properties, however, the significance of a third parameter, namely the surface chemistry at the nanoscale level, is by now a recognized means of tuning the adsorption capacity of the pore network. The affinity between the carbon surface and the fluid phase plays a major role in adsorption processes, as the generally non-specific interaction substantially affects the distribution of the adsorbed molecules within the pores. Introduction of heteroatoms into the turbostratic layers renders the carbon surface more attractive to polar molecules. The most common heteroatom in the carbon matrix is oxygen, which generally bonds along the edges of the graphene layers.

This paper investigates the influence on surface wetting of the chemical character of the adsorbent, by modifying the surface chemistry of the sample, in the case of water, which interacts only weakly with graphitic carbon surfaces. Non-polar vapour molecules are attracted to graphene sheets through a strong dispersion interaction, which favours adsorption even at low relative pressures P/P_0, while the adsorption of water on the carbon surface is hindered by the strong hydrogen bonding among the water molecules in the fluid (Dubinin 1980; Mowla et al. 2003). At very low surface coverage water adsorption is governed both by the surface chemistry and the porosity of the carbons. Water uptake at low P/P_0 may thus be enhanced by introducing oxygen functionalities into the carbon, since, through a cooperative bonding mechanism, they have the same effect as

pre-adsorbed water (Muller et al. 1996). Such surface functional groups act as nucleation centres that, upon further accretion, ripen into clusters at P/P_0 as low as 0.1 (Brennan et al. 2001). While pore filling occurs already at low P/P_0 with non-polar adsorbates, for water it does not begin until about $P/P_0 = 0.5$. For higher relative pressures, however, the Dubinin-Astakhov equation is in excellent agreement with the isotherm (Lodewyckx and Vansant 1999).

Under real operating conditions, the ambient relative humidity can place water in competition with other target molecules for adsorption sites, thereby compromising the role of the carbon. For this reason, the recognition of the role of water has a particular relevance in activated carbon-vapour phase interactions.

This paper is based on the complementarity of adsorption and X-ray scattering techniques. The filled status of the pores calculated from adsorption/desorption isotherms depends on the specific adsorption model employed, while small angle X-ray scattering (SAXS) furnishes direct information on the spatial occupation. Pore-filling adsorbed molecules reduce the electron density contrast with the surrounding carbon matrix and thus modify the SAXS signal of the sample. By comparing the modified signal with that of the dry sample, structural information can be deduced about the adsorbed phase (Hoinkis 2004; Mitropoulos et al. 1995; Ramsay 1993; Antxustegi et al. 1998; Lozano-Castelló et al. 2001b). As the SAXS response is related to spatial distances through the transfer wave vector q, the pore-filling by the adsorbed molecules can be conveniently translated into the pore size w as $2\pi/q$. Such observations yield model-independent information about pore filling by any adsorbed molecule.

The present article compares water vapour adsorption and SAXS measurements on activated carbon samples of well characterized surface morphology and chemistry.

2 Experimental

To avoid inorganic impurities from the raw materials, the samples described in this paper were prepared from a polymer precursor and were chemically modified to varying degrees by oxidation with nitric acid. Granular activated carbon (APET) was prepared from poly(ethylene terephthalate) (PET) pellets (Bóta et al. 1997). Steam-activated carbon, obtained at 900 °C, was treated for 3 hours with concentrated nitric acid at room temperature (APETA) and at the boiling point of the carbon–acid suspension (APETB) to achieve different degrees of surface functionalization. Before use, these acidic samples were washed with distilled water and extracted in a Soxhlet apparatus until neutral pH was attained. The surface chemistry and morphology of these carbons have been characterized elsewhere (László et al. 2004, 2005).

Nitrogen adsorption/desorption isotherms, measured at 77 K with a Quantachrome Autosorb-1 instrument, were of Type I, as also discussed previously (László et al. 2004). The surface areas obtained from the BET and the Dubinin-Radushkevich (DR) models for APETA were 1114 and 1293 m^2/g, respectively. For APETB, however, the hot nitric acid treatment reduced the surface area to less than 340 m^2/g, but the pore size distribution (PSD) in the micropore range, as deduced from N_2 adsorption data, nevertheless remained practically unaffected. Average pore widths, derived from the ratio of the total pore volume to the surface area assuming slit shaped geometry, were respectively 8.6 and 9.2 Å for APETA and APETB. The true densities d_{He} of the same samples, determined by helium pycnometry with the same AUTOSORB-1 instrument, were 1.82 and 1.50 g/cm^3. The PSD in the micropore range was deduced from CO_2 adsorption measurements at 273 K performed by the Autosorb instrument, using the DFT/Monte Carlo differential PSD program. Water vapour adsorption isotherms were measured on a volumetric Hydrosorb apparatus (Quantachrome) at 20 °C. The nominal resolution of the instrument is 0.005 mg sorbed water. The equilibration pressure did not change by more than 0.05 mmHg over a period of 60 s. The datum point was taken after 2000 s whether or not the pressure had equilibrated, unless the pressure fell too far from its target value (<0.05% of P_0). The cross-sectional area of water used in the calculations was 12.5 $Å^2$.

XPS analysis of the surface chemistry in the powdered samples (László et al. 2001; László and Geissler 2006) showed a strong increase in the O/C atomic ratio, from 10 to 27%, for APETA and APETB respectively. The close similarity found between the populations of the different functional groups in the granular and the powdered samples is proof that the chemical treatment acted uniformly throughout the internal surfaces. Table 1 lists the surface chemical groups detected by XPCS in the two powdered samples.

SAXS measurements on the BM2 beam line at the European Synchrotron Radiation Facility (ESRF), Grenoble,

Table 1 Analysis of the C1s region of the XPS spectra of the powdered samples (at. %)

Sample	Graphitic carbon	Phenolic, alcohol, ether	Carbonyl, quinone	Carboxyl, ester	Shake-up satellites
APETA	48.8	26.4	11.3	7.9	5.6
APETB	50.9	23.7	6.1	15.3	4.0

France were made at two different wavelengths, $\lambda_0 = 1.57$ and 0.69 Å,with sample-detector distances 158, 27 and 6 cm. An indirect illumination CCD detector (Princeton Instruments) with 50 μm effective pixel size was used. Intensity curves $I(q)$, obtained by azimuthal averaging, were corrected for grid distortion, dark current, sample transmission and variations of the incident beam intensity, as well as for background scattering.

The powdered samples, ground in a ball mill to about 0.3 mm particle size, were inserted into 1.5 mm diameter Lindemann glass capillaries and heated to 110 °C for 24 hours to remove trapped or adsorbed water. The capillaries were equilibrated in air containing water vapour at 11–98% relative humidity (RH) for 8 weeks and then sealed. It is notable that this equilibration time is much longer than that employed to measure a complete gas adsorption cycle (ca. 1 day). Intensities were normalized with respect to a standard (lupolen), assuming an effective sample thickness of 1 mm to account for the filling factor of the powder in the capillary tubes. The SAXS measurements were made at the same temperature as the sample preparation (20 °C).

3 Theoretical background

The intensity of X-rays of wavelength λ scattered through an angle θ by a carbon sample in dry air is governed both by the structure factor of the carbon, $S_1(q)$, and the difference in electron density ρ_C between the carbon and air. Thus,

$$I_1(q) = r_0^2 \rho_C^2 S_1(q). \tag{1}$$

In (1), $r_0 = e^2\mu_0/4\pi m$ is the classical radius of the electron, e and m being respectively the electron charge and mass and μ_0 the magnetic permittivity of space. The magnitude of the transfer wave vector for X-rays is $q = (4\pi/\lambda)\sin(\theta/2)$. The electron density of the carbon is

$$\rho_C = Z d_{He} N_A / M, \tag{2}$$

where Z is the atomic number, M the atomic mass, d_{He} the helium density of the sample and N_A Avogadro's number. The presence of light heteroatoms such as oxygen does not alter the above definition of the electron density of the carbon, as their ratio Z/M is identical. Only the helium density d_{He} is affected by their presence. Although the same argument does not apply to hydrogen owing to its larger value of Z/M, its contribution is negligible since it contains few electrons. The value of $\rho_C$is therefore determined essentially by the mass density of the carbon. In (1) the electron density of the surrounding air does not appear as it is much smaller than ρ_C.

If the sample is impregnated with a fluid that does not completely fill all the unoccupied space in the carbon, the expression for the scattered intensity becomes that of a ternary system, namely

$$I_{tern}(q) = r_0^2\{(\rho_C - \rho_l)^2 S_{cl}(q) + \rho_C^2 S_{cv}(q) + 2\rho_C(\rho_C - \rho_l) S_{lv}(q)\} \tag{3}$$

where $S_{cl}(q)$ is the partial structure factor describing the relative positions of carbon and liquid, $S_{cv}(q)$ that between carbon and vapour phase, while $S_{lv}(q)$ is that between liquid and vapour phase. Far from critical conditions, the electron density of the vapour phase is negligible with respect to that of the liquid and so is equivalent to a vacuum. Owing to the dispersed nature of micropores in carbons, however, in many cases the effective liquid-vapour interface is very small and regions in the carbon in which the fluid is adsorbed are physically separated from those in which only the vapour phase is present. In such a case the last term in (3) is negligible and the first two terms can be represented by a pseudo-binary expression of the form

$$I_2(q) = r_0^2(\rho_C - \rho_S)^2 S_2(q) \tag{4}$$

in which it is understood that the $(\rho_C - \rho_S)^2 S_2(q)$ is an average over the regions in the sample where the fluid is adsorbed and where it is not. Since these two regions generally have different characteristic sizes and therefore contribute to different zones in q-space, it is reasonable to attribute a q-dependence to ρ_S, i.e., $\rho_S(q) = p(q)\rho_l$, where ρ_l is the density of the adsorbed fluid and $p(q)$ is the relative electronic (or mass) density of the fluid with respect to its bulk value. Provided the fluid does not alter the structure of the carbon, $S_1(q)$ and $S_2(q)$ both describe the same total structure factor of the carbon and hence $S_1(q) = S_2(q)$. If the pores are uniformly filled then the two signals $I_1(q)$ and $I_2(q)$ are everywhere proportional to each other, i.e., ρ_S and $p(q)$ are independent of q. If, however, the fluid is not uniformly distributed, e.g., molecules adsorb only in the finest pores while remaining in the vapour state elsewhere, then the deviations from uniform filling may be expressed by the intensity ratio

$$u(q) = I_2(q)/I_1(q) = [\rho_C - p(q)\rho_l]^2/\rho_C^2, \tag{5}$$

from which it follows that

$$p(q) = \rho_C[1 - u(q)^{1/2}]/\rho_S. \tag{6}$$

In principle, $0 \le p(q) < 1$ when the pores are incompletely filled, but $p(q)$ can exceed unity if a strong interaction exists between the surface and the adsorbed layer. $p(q)$ is thus a direct measure in reciprocal space of the relative density of the adsorbed molecules with respect to the bulk liquid. In this model-independent approach, the two basic requirements are that the carbon structure should not be altered by

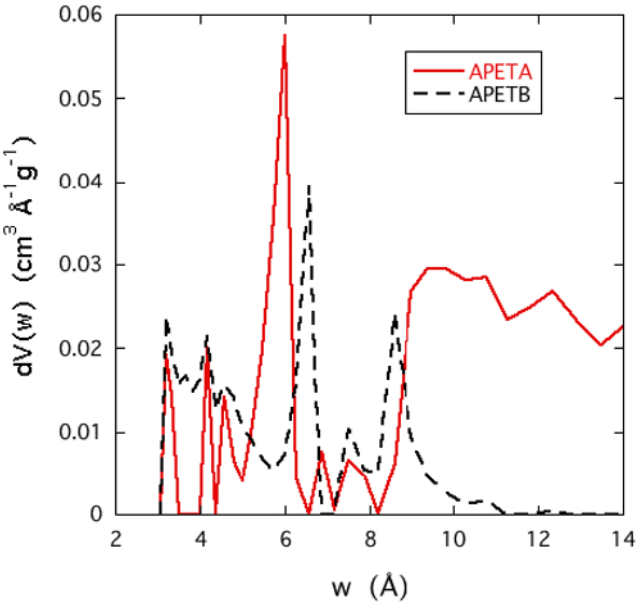

Fig. 1 Pore size distribution in the ultra-micropore range derived from CO_2 adsorption data at 273 K for the samples APETA and APETB

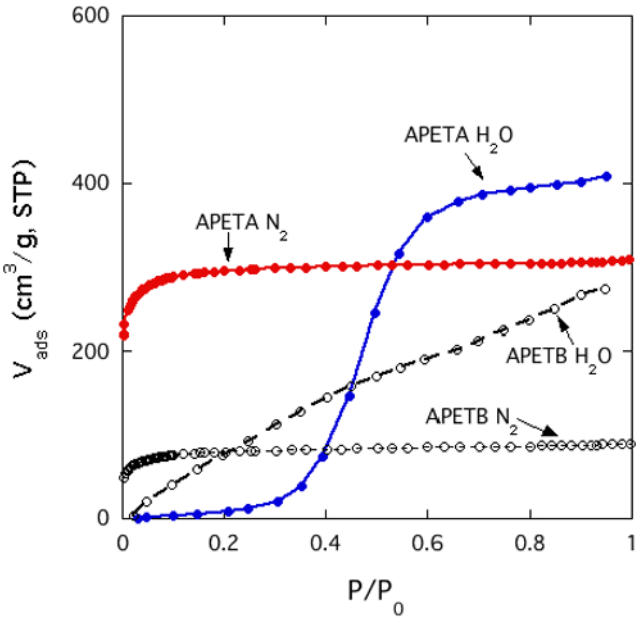

Fig. 2 Adsorption isotherms for water at 20 °C and nitrogen at 77 K for the samples APETA and APETB

the adsorbed molecules, and that the test sample and the dry reference should be equivalent. Apparently negative values of $p(q)$ may arise if the adsorbent causes structural changes ($S_1(q) \neq S_2(q)$), or also if the reference sample is contaminated. Strongly negative values of $p(q)$, however, can occur if extended regions of contact exist between the condensed liquid phase and its vapour. This extra scattering, corresponding to the third term in (3), is neglected in the above pseudo-binary model of independent scattering regions and is an indicator of cluster or droplet formation in the sample. In this case, to determine the partial structure factors of (3), contrast variation techniques are required, for instance by solvent deuteration with SANS, or anomalous scattering with SAXS. As, however, perturbations from the ternary component tend to be confined to low values of q, the binary model can retain its validity in certain regions of reciprocal space.

4 Results and discussion

Figure 1 reveals that APETB retains strong microporous character and that the details of the CO_2 PSD below 9 Å differ only slightly from those of APETA. In Fig. 2 the water vapour adsorption isotherms of the two carbon samples are displayed and compared with those of nitrogen at 77 K. For nitrogen, both samples exhibit isotherms of Type I, while with water vapour APETA displays an isotherm of Type V, owing to the weak interaction between the graphene layers and the water, as a result of the small number of polar sites. Adsorption increases at $P/P_0 \approx 0.3$ and a wide plateau develops above $P/P_0 \approx 0.6$. On the basis of the observation of Dubinin, namely that on nonpolar carbon surfaces a water monolayer develops at this relative pressure, a BET surface area S_A of 1310 m^2/g in contact with monolayer water can be deduced.

Table 2 Characteristic data derived from the nitrogen (77 K) and water (293 K) adsorption data

			APETA	APETB
$V_{tot}(P/P_0 \rightarrow 0.99)$	cm^3/g	N_2	0.50	0.14
		H_2O	0.44	0.24
S_A	m^2/g	N_2	1114	304
		H_2O	1312*	426**

*Assuming that at $P/P_0 \approx 0.6$ a monolayer of water develops; ** From BET model

The hot nitric acid treatment results in a threefold increase in the surface oxygen concentration, which transforms the water vapour isotherm of APETB from concave to convex shape (the value of the C parameter of the BET equation is 4): the introduced oxygen functionalities, especially the carboxylic groups, increase the affinity for water of the carbon surface. This water vapour curve was found to be reproducible. Some data from the nitrogen and water adsorption are compared in Table 2. The Gurvitsch rule is not obeyed. In APETA water gives a smaller total pore volume V_{tot} than nitrogen. According to Gregg and Sing (1982), this may partly be because the density of water in the pores is lower than that of liquid water at the same temperature, as indeed is suggested by the SAXS results described below. The discrepancy, however, cannot be attributed to in-

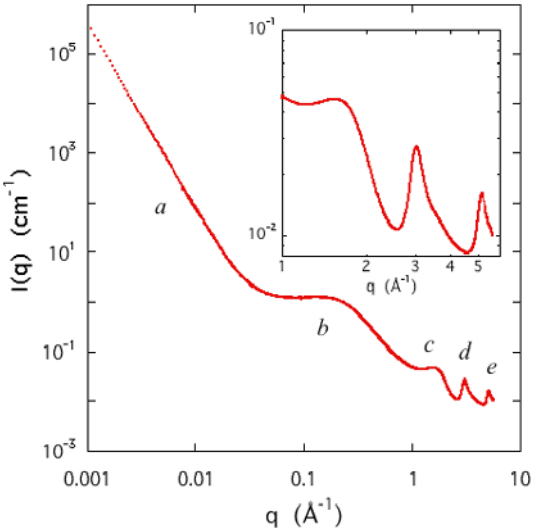

Fig. 3 SAXS spectrum of dry sample APETA with regions *a–e* described in the text. *Inset* shows WAXS region (zones *c–e*) where the absence of Bragg reflections indicates that the carbon is amorphous

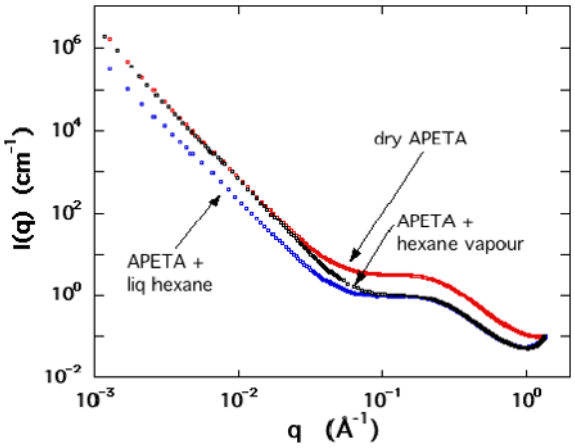

Fig. 4 Scattering spectra of APETA in air, in hexane vapour and in liquid hexane

trinsic closed pores, since with hexane vapour, the fraction of closed pores in this sample was found to be negligible (László and Geissler 2006). We conclude therefore that the effect is the result of poor wettability and induced pore inaccessibility caused by blocking with water molecules. The more pronounced discrepancy in the case of APETB is also a result of several effects. The narrowest pores at 77 K are inaccessible for the N_2 molecules. Due to the heavy acidic treatment the pore walls are flexible, as this carbon exhibits low pressure hysteresis with nitrogen. For the smaller water molecules with their higher kinetic energy, access is enhanced. Moreover, the wettability of the surface is promoted by the oxidative treatment. Finally, as the number of functional groups is much greater, oriented adsorption of the water molecules may take place, which increases the probability of multilayer formation as $P/P_0 \to 0.99$.

Figure 3 exemplifies a typical SAXS spectrum from a dry sample (APETA), measured on the BM2 instrument. Five features are illustrated. In region *a* at low q, the spectrum is dominated by surface scattering from grain boundaries within the powder particles. The size of the constituent grains is approximately 1 μm (László et al. 2004) and the power-law behaviour visible here, $I(q) \propto q^{-4}$, is attributable to scattering from smooth interfaces (Porod 1982). In region *b* scattering comes from the microporous structure. The slope to the right of the shoulder is identified with surface scattering from the high internal surface area of the carbon (László et al. 2004; László and Geissler 2006). The broad peaks labelled *c*, *d* and *e* located in the conventional wide angle X-ray scattering (WAXS) range, enlarged in the inset of Fig. 3, are residues of the main diffraction peaks of graphite (Bernal 1924), in which the long range order is replaced by short range liquid-like order. The absence of sharp diffraction peaks in this region signifies that the sample is free from microcrystalline graphite or impurities.

The principle of SAXS combined with contrast variation technique is illustrated by the example of APETA with a highly wetting liquid, n-hexane. Figure 4 compares three SAXS responses, from a dry sample, a sample exposed to hexane vapour ($P/P_0 = 0.4$) and one immersed in liquid hexane, respectively. In the higher-q regions the intensities scattered by the vapour and liquid samples are superimposed and are weaker than the dry sample, indicating that hexane is adsorbed in the finer pores. In the lower q-range the opposite is true, as the curves of the hexane vapour and the dry sample coincide. In the larger pores and in the grain boundaries, therefore, no condensation occurs. By contrast, filling is complete at all distance scales in the sample in contact with liquid hexane.

It was shown recently that the pseudo-binary model appears to give a consistent qualitative description of pore filling in carbons of different surface chemistry for n-hexane (László and Geissler 2006). There is, however, a need for a systematic SAXS study of samples in contact with water vapour in a wide range of RH as well as for a comparison with vapour adsorption measurements.

Figure 5a shows SAXS results from the lightly oxidized sample APETA in the dry state and with water vapour. Several features are notable. In the range $0.2 < q < 2.1$ Å^{-1}, (i.e., in the distance range $30 > d > 3$ Å, where $d = 2\pi/q$) the curves from the humid samples lie below that of the dry curve. This means that condensation occurs in the micropores. The decrease in intensity is not monotonic, however, as a much larger change in intensity occurs between 33 and 43% RH than between 0 and 33% RH. Secondly, at high q, the curves meet at $q \approx 2.1$ Å^{-1}, implying that the smallest space in the carbon structure into which the water molecules can penetrate is $d_{crit} \approx 3.0$ Å, in reasonable agreement with the known critical size of the water molecule, 2.92 Å (Webster et al. 1998). This numerical value,

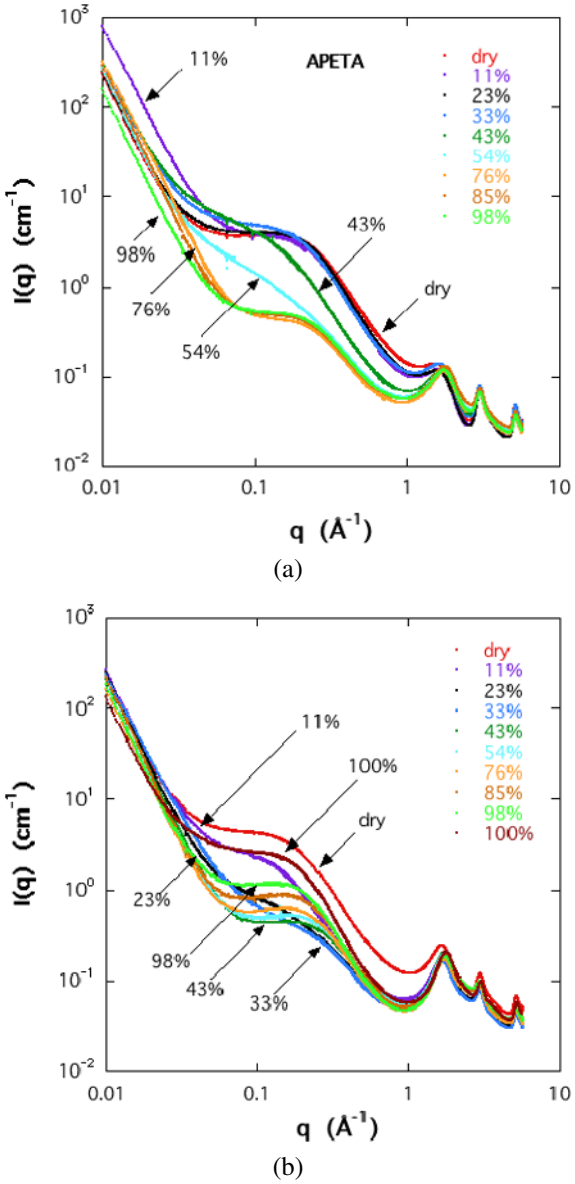

Fig. 5 (Color online) (**a**) Scattering curves for APETA in the dry state and in water vapour at different RH. At low q the intensity scattered by the humid samples surpasses that of the dry sample, indicating cluster formation. (**b**) Scattering curves for APETB in the dry state and in water vapour at different RH. The intensity of the saddle at $q \approx 0.1$ Å^{-1} decreases monotonically until RH = 45%, then increases again due to liquid-vapour interfaces

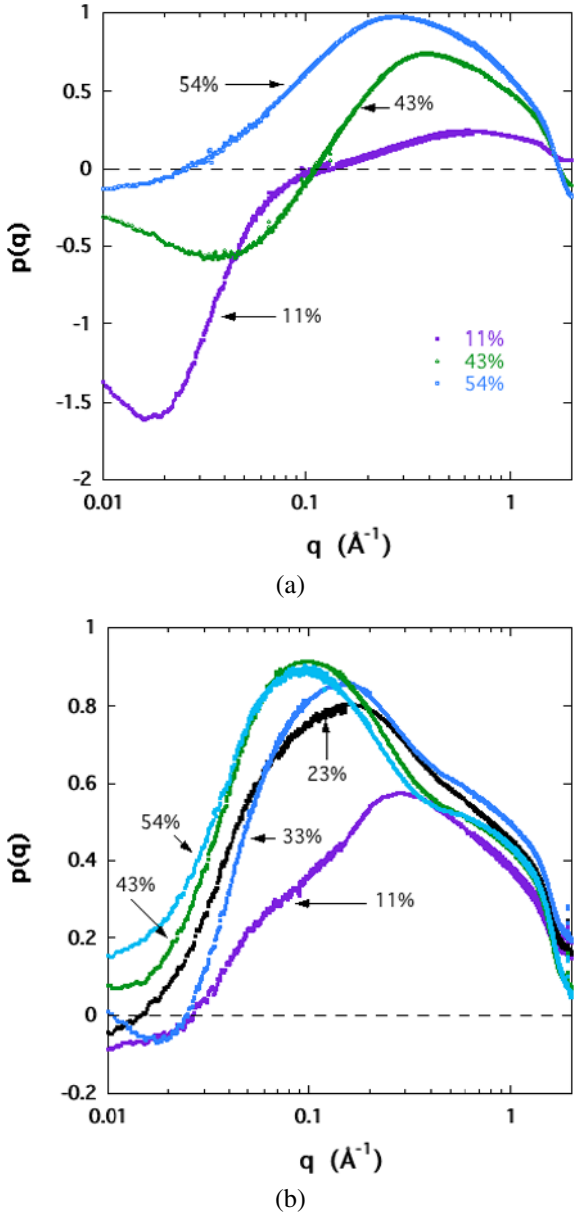

Fig. 6 (**a**) Density function $p(q)$ of water in APETA for three values of RH, 11, 43 and 56%, calculated from (6). For clarity, only 20% of the data are shown. (**b**) Density function $p(q)$ for water in APETB at 5 values of RH, calculated from (6). For clarity, only 20% of the data are shown

however, should be viewed with caution, since corrections for scattering from the adsorbed water become significant in this region. Thirdly, at $q < 0.2$ Å^{-1}, the scattering intensity from the humid samples *exceeds* that in the dry system, in contradiction with (5) and (6). The source of this extra scattering is the neglected third term in (3), which describes correlation between adsorbed water and its vapour. As already stated, the extra scattering appears as a negative region in the density function $p(q)$. The variation of $p(q)$ displayed in Fig. 5 shows that at low RH small amounts of water adsorb initially in the micropores, while strong cluster formation develops on the more open surfaces. It is important, however, to point out that to appreciate the actual *volume* of liquid contributing to these features, the values of $p(q)$ must be weighted by q^2. Since the scattering from clusters contributes essentially at small values of q, it follows that the volume occupied by the droplets is much smaller than that in the micropores.

Above 43% RH the amount of adsorbed water in the micropores starts to increase significantly, as also confirmed by the water isotherm. The shape of the density functions in the

higher q range seems to suggest a bimodal distribution of the populated pores. Although attempts can be made to estimate the contribution from the clusters, the full partial structure factors in (3) can be solved only with the aid of contrast variation methods such as are afforded by small angle neutron scattering. Unlike the present experiment where the vapour pressure is varied, such measurements involve varying the scattering density ρ_l by means of hydrogen/deuterium substitution at constant vapour pressure. This type of measurement lies outside the scope of the present investigation.

The density function $p(q)$ of water adsorbed in APETB has a different appearance from that of APETA. At the high-q end of the spectrum a shoulder appears, displaying a maximum height of about 0.6. The bimodal distribution suspected in APETA becomes more clearly resolved with increasing RH. Negative-going values of $p(q)$, discernable at low q, are much less pronounced than in APETA. This observation, however, by no means implies that droplet formation is absent: on the contrary, the increase in the height of the saddle feature at 0.1 Å^{-1} for RH > 0.54 is an unmistakable signature of clusters.

To establish a quantitative comparison between the macroscopic isotherms and the SAXS results, perturbations from liquid-vapour interfaces should be minimized. To this end, we restrict attention to the higher q-range of the spectrum, where the ratio of the liquid/vapour interfacial area to that of the solid/liquid or solid/vapour is small. In the Porod approach, the intensity scattered by the pore surfaces at the high-q end of the SAXS spectrum (final slope method) is proportional to the surface area of the sample S/V (Porod 1982). Thus

$$I(q) = Kq^{-4} + b, \tag{7}$$

where $K = 2\pi[\rho_C - p(q)\rho_s]^2 S/V$ and b is a constant that simulates the signal from the atomic disorder in the sample. The data from the region of scattering from pores should therefore display straight line behaviour when plotted in the form

$$I(q)q^4 = K + bq^4 \tag{8}$$

Figure 7 shows the results from the Porod scattering region for different RH, from which the values of the intercept K are obtained. The corresponding expression for $p(q)$ in this high-q range is obtained by analogy with (6). Thus

$$p(\infty) = \rho_C[1 - (K/K_{dry})^{1/2}]/\rho_S \tag{9}$$

where K_{dry} is the "final slope" of the reference sample and K that of the sample exposed to water vapour. (For brevity the symbol ∞ is used here to designate the high-q region $0.6 < q < 1$ Å^{-1} from which the values of K are determined.)

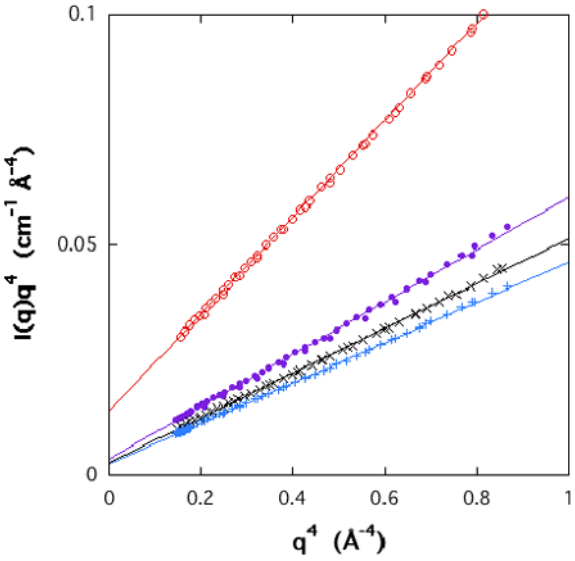

Fig. 7 Plots of scattering intensity $I(q)q^4$ versus q^4 from sample APETB for RH = 0% (*open circles*), 11% (*filled symbols*), 23% (×) and 33% (+). The intercepts yield the value of K

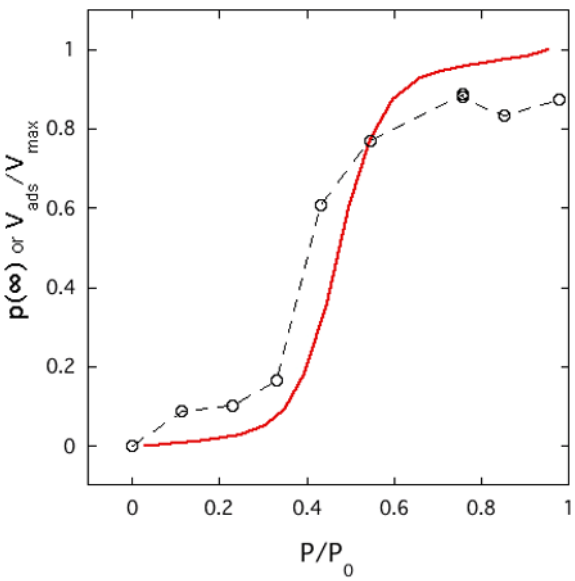

Fig. 8 Normalized H_2O adsorption isotherms for APETA with respect to the maximum adsorption, compared with $p(q)$ (*open circles*) from the final slope region ($0.6 < q < 1$ Å^{-1}). Even at the highest P/P_0 the smallest micropores ($8.4 \leq w \leq 10$ Å) are incompletely filled

Figures 8 and 9 compare the SAXS measurements of adsorption of water vapour in the microporous region and the adsorption isotherms, normalized with respect to the maximum adsorption. In APETA the same trend is observed between these two different measurements, with, however an initial step of $p(\infty) \approx 0.1$ that is not replicated in the isotherm. It seems probable that the difference in these responses is due to the different conditions of sample preparation, notably the exposure time to the H_2O vapour and

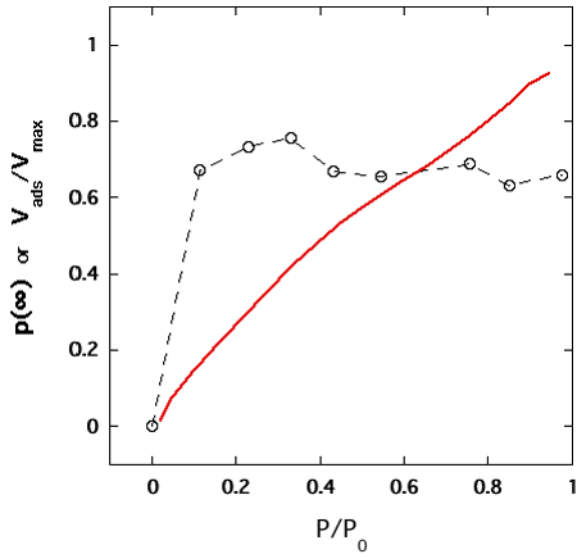

Fig. 9 Normalized H_2O adsorption isotherms for APETB, compared with $p(q)$ (*open circles*) calculated from the final slope region ($0.6 < q < 1$ Å^{-1}). For $P/P_0 \geq 0.11$ the density of the adsorbed water in the micropores is essentially constant. *Dashed lines* are guides for the eye

its concentration. The adsorption measurements on the Hydrosorb instrument were made with vapour generated at 100 °C in a few hours, while the SAXS samples were exposed to water vapour of various RH at 20 °C for two months. For APETB, the difference between the two observations is even more marked. The equilibrium value of $p(\infty)$ appears to be independent of RH over the whole range explored, while the adsorption isotherm reveals a much more gradual behaviour. Once again, these results indicate that slow rearrangements of the adsorbed H_2O vapour occur within the carbon, possibly combined with ageing of the surface functional groups. It is also remarkable that the maximum density of water is greater in APETA than in APETB. This finding suggests that in the latter case access to the pores may be blocked by water molecules adsorbed on functional groups located at the entrance of the pores, thus hindering the passage of further adsorbates. The shape of all the SAXS curves reflects a complex distribution that is at least bimodal.

5 Conclusions

Activated carbons investigated by small angle X-ray scattering displayed significant differences in the way water vapour is adsorbed that depend on their prior surface-treatment. Lightly oxidized samples (APETA) display significant cluster formation in the macroporous region, while in the heavily oxidized sample (APETB) cluster formation is more limited. In the latter, pore filling by water is constant over the whole range of RH explored (0–98%) and does not exceed about 70%. Micropore filling in the more lightly oxidized sample, however, tends to mimic the adsorption isotherm. At high relative pressure, it is greater than in APETB, an effect that is attributed to steric hindrance by water clusters around functional groups at the entrance to the pores. Differences between the adsorption isotherms and the SAXS results are attributed to the effects of rearrangement and/or ageing in the sample.

Nomenclature

θ	Scattering angle
λ	Wavelength of the scattered X-ray, Å
μ_0	Magnetic permittivity of space, N/Å^2
λ_0	Wavelength of the incident X-ray, Å
ρ_C	Electron density of carbon, cm^{-3}
ρ_l	Electron density of the condensed liquid, cm^{-3}
ρ_S	Electron density of the sample, cm^{-3}
b	Constant
C	Parameter of the BET equation
d	Diameter of pores, Å
d_{crit}	Critical size of molecules, Å
d_{He}	Density measured by helium pycnometry, g/cm^3
e	Electron charge, C
$I(q)$	Intensity of the scattered X-rays
K	Slope of $I(q)$ vs. q^{-4}
K_{dry}	Final slope of $I(q)$ vs. q^{-4} of the reference sample
m	Electron mass, g
M	Atomic mass
$p(\infty)$	Relative density of the fluid with respect to the bulk value in the high-q region $0.6 < q < 1$ Å^{-1}
$p(q)$	Relative density of the fluid with respect to the bulk value
P/P_0	Relative pressure
q	Transfer wave vector, Å^{-1}
r_0	Classical radius of electron, m
RH	Relative humidity, %
S	Surface area of the sample, m^2
S_A	BET surface area, m^2/g
$S_{cl}(q)$	Partial structure factor between carbon and liquid phase
$S_{cv}(q)$	Partial structure factor between carbon and vapour phase
$S_i(q)$	Structure factor of material i
$S_{lv}(q)$	Partial structure factor between liquid and vapour phase
V	Volume of the sample, m^3
V_{tot}	Total pore volume at $P/P_0 \rightarrow 1$, cm^3/g
w	Pore width, nm
Z	Atomic Number

Acknowledgements The European Synchrotron Radiation Facility is gratefully acknowledged for access to the small angle beamline BM2. We express our thanks to G. Bosznai and J.F. Bérar for their invaluable assistance. This research was supported by the EU–Hungarian Government joint fund (GVOP-3.2.2-2004-07-0006/3.0).

References

Antxustegi, M.M., Hall, P.J., Calo, J.M.: Development of porosity in Pittsburgh No. 8 coal char as investigated by contrast-matching small-angle neutron scattering and gas adsorption techniques. Energy Fuels **12**, 542–546 (1998)

Bernal, J.D.: The structure of graphite. Proc. R. Soc. Lond., A Contain. Pap. Math. Phys. Character **106**(740), 749–773 (1924)

Bóta, A., László, K., Nagy, L.G., Copitzky, T.A.: Comparative study of active carbons from different precursors. Langmuir **13**, 6502–6509 (1997)

Brennan, J.K., Bandosz, T.J., Thomson, K.T., Gubbins, K.E.: Water in porous carbons. Colloids Surf. A **187–188**, 539–568 (2001)

Dash, R.K., Yushin, G., Gogotsi, Y.: Synthesis, structure and porosity analysis of microporous and mesoporous carbon derived from zirconium carbide. Microporous Mesoporous Mater. **86**(1–3), 50–57 (2005)

Dubinin, M.M.: Water-vapor adsorption and microporous structures of carbonaceous adsorbents. Carbon **18**, 355–364 (1980)

Gregg, S.J., Sing, K.S.: Adsorption, Surface Area and Porosity. Academic Press, London (1982)

Hoinkis, E.: Small-angle scattering studies of adsorption and of capillary condensation in porous solids. Part. Part. Syst. Charact. **21**, 80–100 (2004)

László, K., Geissler, E.: Surface chemistry and contrast-modified SAXS in polymer-based activated carbons. Carbon **44**, 2437–2444 (2006)

László, K., Tombácz, E., Josepovits, K.: Effect of activation on the surface chemistry of carbons from polymer precursors. Carbon **39**(8), 1217–1228 (2001)

László, K., Marthi, K., Rochas, C., Ehrburger-Dolle, F., Livet, F., Geissler, E.: Morphological investigation of chemically treated PET-based activated carbons. Langmuir **20**, 1321–1328 (2004)

László, K., Czakkel, O., Josepovits, K., Rochas, C., Geissler, E.: Influence of surface chemistry on the SAXS response of polymer-based activated carbons. Langmuir **21**, 8443–8451 (2005)

Lillo-Ródenas, M.A., Lozano-Castelló, D., Cazorla-Amorós, D., Linares-Solano, A.: Preparation of activated carbons from Spanish anthracite: II. Activation by NaOH. Carbon **39**(5), 751–759 (2001)

Lodewyckx, P., Vansant, E.F.: Water isotherms of activated carbons with small amounts of surface oxygen. Carbon **37**, 1647–1649 (1999)

Lozano-Castelló, D.M., Lillo-Ródenas, A., Cazorla-Amorós, D., Linares-Solano, A.: Preparation of activated carbons from Spanish anthracite: I. Activation by KOH. Carbon **39**(5), 741–749 (2001a)

Lozano-Castelló, D., Cazorla-Amorós, D., Linares-Solano, A., Hall, P.J., Gascon, D., Galan, C.: In situ small angle neutron scattering study of CD_4 adsorption under pressure in activated carbons. Carbon **39**, 1343–1354 (2001b)

Mitropoulos, A.C., Haynes, J.M., Richardson, R.M., Kanellopoulos, N.K.: Characterization of porous glass by adsorption of dibromomethane in conjunction with small-angle X-ray scattering. Phys. Rev. B **52**, 10035–10042 (1995)

Mowla, D., Do, D.D., Kaneko, K.: Adsorption of water vapour on activated carbon. In: Radovic, L.R. (ed.) Chemistry and Physics of Carbon, vol. 28, pp. 230–262. Dekker, New York (2003)

Muller, E.A., Rull, L.F., Vega, L.F., Gubbins, K.E.: Adsorption of water on activated carbons: A molecular simulation study. J. Phys. Chem. **100**, 1189–1196 (1996)

Porod, G.:. In: Kratky, O., Glatter, O. (ed.) Small Angle X-ray Scattering. Academic Press, New York (1982)

Ramsay, J.D.F.: Applications of neutron scattering in investigations of adsorption processes in porous materials. Pure Appl. Chem. **65**(10), 2169–2174 (1993)

Webster, C.E., Drago, R.S., Zerner, M.C.: Molecular dimensions for adsorptives. J. Am. Chem. Soc. **120**, 5509–5516 (1998)